An experimental study of the crater evolution by impact of a drop onto a fluctuating shallow pool

N. P. van Hinsberg*, I. V. Roisman and C. Tropea
Chair of Fluid Mechanics and Aerodynamics
Technische Universität Darmstadt
64287 Darmstadt, Germany

Abstract

In this paper experimental investigations of a normal drop impact onto an oscillating liquid film of a finite thickness are performed. The liquids used in the experiments are distilled water, isopropanol and a mixture of glycerine and water and the impact occurs in ambient air. The shape of the crater formed upon the impact is observed using the high-speed video system. The effects of different drop impact velocities, physical properties of the liquids (surface tension and viscosity), different fluctuating film frequencies and amplitudes, on the time evolution of the crater formed within the film upon impact are investigated. Using the experimental results, the dynamics of drop impact on liquid surfaces is analyzed, focusing on the depth and diameter of the crater, and comparing the measurements to a drop impact onto a steady film, under the same conditions. This comparison reveals whether the oscillating film has any influence on the cavity formed after impact.

Introduction

Spray impact and drop impact onto a liquid film is encountered frequently in nature and leads to different phenomena like air bubble formation during heavy rain, formation of a crown-like liquid sheet (so-called corona) with detaching secondary droplets, drop-to-drop, drop-to-corona and corona-to-corona interactions. Drop impact onto liquid films has also importance in various engineering fields. It is important in soil erosion, in agriculture for the dispersion of seed and microorganisms and in many other technical applications such as spray coating and cooling, paint-spraying, criminal forensics, and internal combustion engines with direct fuel injection, where the fuel is sprayed into engine cylinders in the form of small droplets which impact on the inner walls of cylinders [1-4]. Furthermore, spray impact is common in atmospheric sciences for separation of electrical charges by the liquid disintegration during splashing [5], as well as in rainwater separation in water boxes in air-conditioning systems in automobiles [6].

Many coatings of solid substrates are achieved by means of sprays; for example, spray painting [7, 8]. The aim is to achieve a more regular and homogeneous coating. In this context, the impact of a single drop onto a smooth and horizontal solid surface or liquid film has often been used as the simplest system simulating the spray process, by applying superposition of single drop impact events onto a steady liquid film [9-11]. However, sprays impacting onto a substrate create on it a thin, moving, fluctuating liquid film. Because of the wavy and moving surface of this film, a comparison with single drop impact on a steady liquid surface is not valid anymore. To build a bridge between single drop impact onto a film on one side and spray impact onto a moving liquid film on the other side, we present here experiments of a single normal drop impact onto a oscillating film of finite thickness.

The formation and evolution of the crater formed upon the impact beneath the surface are investigated at various film thicknesses, drop impact velocities, liquids properties, and for different fluctuating film frequencies and amplitudes. These results are compared with those of single drop impact onto a steady film [12-13], in order to investigate the influence of an oscillating film on the cavity formed after impact.

Materials and Methods

Experimental measurements were performed using the experimental setup shown in Figure 1. Drops are generated using a medical syringe pump which is programmed to dispense the liquid at a constant flow rate of about 0.40 l/s - 1.81 l/s, depending on the fluid used. The drop is formed and grows at the tip of the needle until its weight exceeds the net upward surface tension force on the drop and the drop detaches from the needle. The rate at which drops grow and fall can be changed by adjusting the speed of the stepping motor of the push-pull syringe pump. The

*nvanhinsberg@sla.tu-darmstadt.de

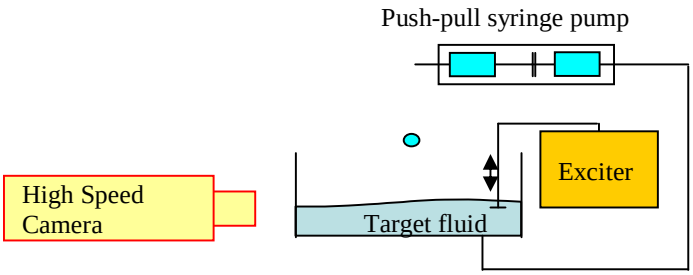

Figure 1. Experimental setup

falling drops are enclosed in a vertical 32 mm Perspex tube to protect them from air flow disturbances. The drops pass a light barrier before falling into the centre of a Perspex cylinder of 90 mm diameter used to hold the target liquid. The fluid of the drops and the target liquid are the same for each experiment. In order to investigate the influence of a moving and fluctuating film, a small aluminium plate is connected to a vibration exciter Type 4809 (Brüel & Kjær) which allows a peak to peak vibration amplitude between 0 and 8 mm and a frequency range of 10 Hz to 20 kHz. The exciter is controlled by a power amplifier, Type 2718 (Brüel & Kjær), as well as by a function generator, Type MXG-9810 (Voltcraft), to set the correct amplitude and frequency respectively.

When the drop passes the light barrier, it activates an electronic delay circuit that triggers the imaging system, consisting of a high-speed camera (Photron Fastcam SA1.1 model 675K-M1), backlit by a continuous light source (Esprit 1500, Bowens). This camera is focussed at the free surface of the target liquid, equipped with an extended 50 mm Cosimar Television lens for a good balance between the required spatial resolution and the necessary field of view, and aligned with the free surface.

Comparison of different cases is enabled by the use of the corresponding non-dimensional numbers governing the impact process: Weber number, $We=\rho U^2 D/\sigma$, giving the relation of inertial to surface tension forces, Ohnesorge number, $Oh=\mu/(\rho\sigma D)^{0.5}$, giving the relation of viscous to surface tension forces, dimensionless film thickness $H=h/D$ and dimensionless time $T=tU/D$. In the above expressions μ, σ and ρ and are dynamic viscosity, surface tension coefficient and density of the liquids used, D and U are the diameter and the impact velocity of the drop, h is the initial film thickness and t the time (set to zero at the first contact between impacting drop and surface).

In order to investigate the influence of the liquid properties on the crater evolution, three liquids were used in experiments: distilled water, isopropanol and glycerin/water mixture consisting of 70% glycerin and 30% water. The initial drop diameter is 2.95 ± 0.01 mm for distilled water, 2.17 ± 0.01 mm for isopropanol and 2.65 ± 0.01 mm for glycerin/water mixture. The drop impact velocity (velocity just before the drop reaches the film surface) is calculated from a distance measurement and a preset time delay between subsequent exposures. Thus, for distilled water the impact velocity varied from 1.68 ± 0.01 *m/s* and 2.88 ± 0.02 *m/s*, for isopropanol from 1.65 ± 0.01 *m/s* to 2.74 ± 0.02 *m/s* and for glycerin/water mixture from 1.82 ± 0.01 *m/s* to 3.06 ± 0.01 *m/s*. The liquid film thickness was varied for all liquids, yielding the non-dimensional film thickness of 0.5 to 2. The film thickness is held perfectly constant by means of the push-pull syringe pump, which sucks the same amount of liquid from the film as is added by the impacting drops. For all drop impacts, the frequency and the amplitude are set to 12 Hz and 980 µm respectively. For glycerine/water additional measurements are performed to investigate the influence of the exciter frequency and amplitude on the crater shape. The physical properties of liquids and ranges of the non-dimensional numbers and exciter settings are given in Table 1.

Table 1. Physical properties of the liquids used (at 20ºC) and the ranges of non-dimensional numbers

	Distilled water	Isopropanol	Glycerin/Water
Density ρ [kg/m^3]	999	805	1179
Viscosity μ [Ns/m^2]	$9.9\cdot10^{-4}$	$2.3\cdot10^{-3}$	$1.86\cdot10^{-2}$
Surface tension σ [N/m]	$7.27\cdot10^{-2}$	$2.36\cdot10^{-2}$	$6.68\cdot10^{-2}$
Ohnesorge number *Oh [-]*	0.0021	0,0113	0.0406
Weber number *We [-]*	112 – 146	199 – 559	151 – 447
Reynolds number *Re [-]*	4,900 – 8,700	1,200 – 2,100	300 – 500
Film thickness *H [-]*	0.5 – 2.0	0.5 – 2.0	0.5 – 2.0
Exciter frequency f_e [Hz]	12	12	1 – 16
Exciter amplitude L_e [µm]	980	980	20 – 1,700
Recording frequency *f [kHz]*	3.6 – 8.0	4.5 – 8.0	4.5 – 8.0

Results and Discussion

A comparison between drop impact onto a steady, non-moving film and an oscillating film at different times for H = 2.0 is given in Figure 2 for the glycerin/water mixture and in Figure 3 for isopropanol. Immediately upon impact, a small circumferential free liquid jet is directed upward. The geometry of this free jet (its height, shape and thickness) depends on the drop impact velocity, liquid properties, liquid film thickness and liquid film movement [12]. For the case of drop impact onto a steady, non-moving film, this free jet is more or less axisymmetric, as the drop impacts orthogonally onto the liquid film and the kinetic energy, needed to direct this free liquid jet upward, is distributed uniformly (Fig. 2 (a) and 3 (a)). In case of impact onto a moving, oscillating film, kinetic energy is constantly pumped into the liquid film, making the surface of the film wavy. As the frequency of the exciter is set to 12 Hz, and the time scale for the first stages of impact are in the order of 1 ms, the impact on the moving, oscillating film can be seen as quasi-steady, resulting into a static inclined drop impact. Depending on the drop impact velocity and the phase of the wave at the exact moment at which the drop impacts, we have seen different free liquid jet shapes appearing, for example an inclined liquid jet, which changes its inclination as time prolongs, or a very asymmetrical liquid jet, consisting of two large curved finger-like jets (Fig. 3 (b)).

Inside the liquid film, the drop impact leads to the formation of a cavity (crater), which penetrates into the film and simultaneously expands radially. During the spreading period inertial forces are dominant over viscous and capillary forces, since the Weber number is much higher than unity. For a quantitative analysis, the crater depth and crater diameter are made dimensionless through division by the drop diameter, and the measured values for the oscillating film are compared to those with a steady film. Here, the depth is measured at the lowest point of the crater, and the diameter at half the film thickness, i.e. for $y = H/2$, where y is the vertical distance measured from the free surface of the film. The time evolution of the dimensionless crater depth and of the symmetry of the crater diameter (measured from the center of the impacting drop) for H = 2.0 are shown in Fig. 4 for glycerine/water, as well as the dimensionless diameter in Fig. 5 for isopropanol. In these graphs, the continued and dashed lines are the measurements for drop impact onto a steady film, whereas the symbols correspond to the oscillating surface. The velocity at which the crater penetrates inside the liquid film is for a steady and for an oscillating film the same, independent of the liquid properties, Weber number and film depth. As the crater approaches the bottom of the film, the first differences can be noticed. For the steady film, at about T = 5 the velocity of the crater depth penetration slows down, and it takes about 10 to 15 dimensionless time steps before the crater reaches the bottom of the film, whereas for the oscillating film, the original penetration velocity remains the same until the crater has reached the bottom (Fig. 4 (a)). The same behaviour is seen for isopropnaol and distilled water (not shown here).

For the change in crater diameter with time, only a slight difference is seen between a steady and an oscillating film, during this growing period of the crater. In general, it can be said that when the film oscillates, the crater diameter is slightly larger at the same time instants. From the moment that the crater reaches the bottom, it can only grow in diameter, until the maximum diameter is reached. This maximum diameter is a function of the film

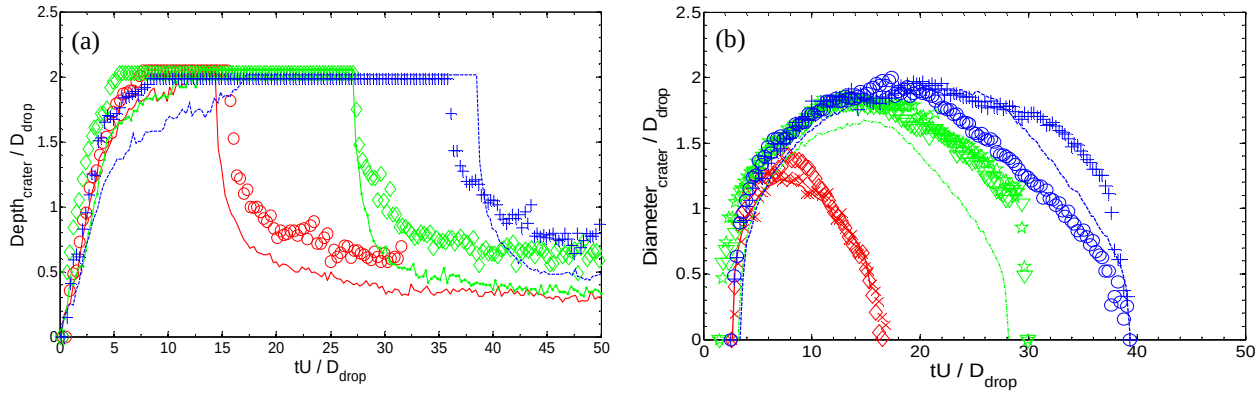

Figure 4. Dimensionless crater depth (a) and symmetry of crater diameter (b) for drop impact of glycerine/water (steady: - H = 2.0, We = 157, Re = 320; -. H = 2.0, We = 308, Re = 434; -- H = 2.0, We = 505, Re = 561; oscillating: (a): ○ H = 2.0, We = 151, Re = 309; ◊ H = 2.0, We = 291, Re = 419; + H = 2.0, We = 444, Re =524; (b): x (left) , ◊ (right) H = 2.0, We = 151, Re = 309; ▽ (left), ☆(right) H = 2.0, We = 291, Re = 419; + (left), o (right) H = 2.0, We = 444, Re =524;)

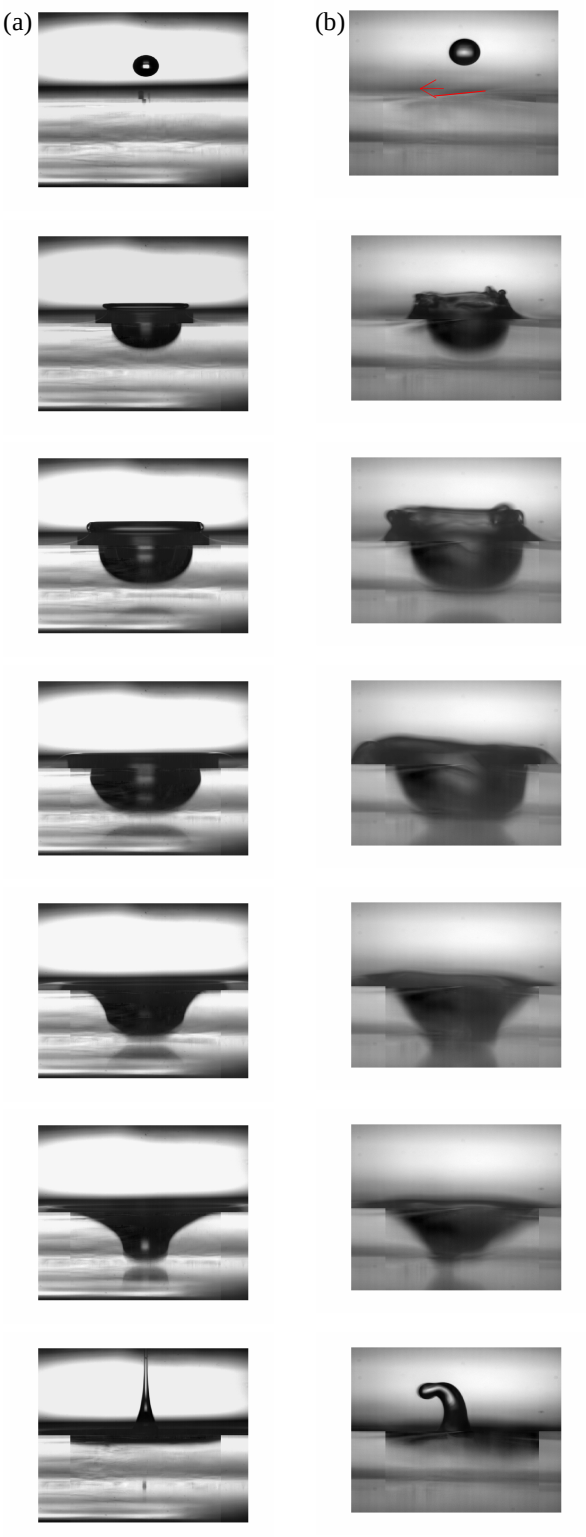

Figure 2. Crater shape for drop impact of Glycerin/water: (a) steady film ($\overline{H}$ = 2, We = 505, Re = 561) and (b) oscillating film ($\overline{H}$ = 2, We = 444, Re = 524), T = -1.04, 3.96, 9.67, 21.95, 30.52, 34.95 and 49.80

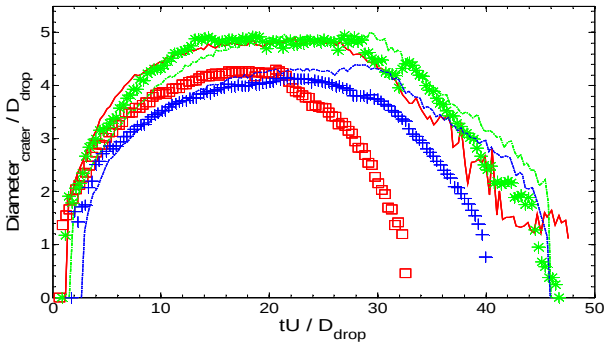

Figure 5. Dimensionless crater diameter for drop impact of isopropanol (steady: - H = 0.5, We = 541, Re = 2010; -. H = 1.0, We = 539, Re = 2010; -- H = 2.0, We = 527, Re = 1980; oscillating: □ H = 0.5, We = 557, Re = 2108; * H = 1.0, We = 558, Re = 2089; + H = 2.0, We = 552, Re =2060)

thickness, liquid properties and Weber number [12-13]. For glycerine/water, the maximum crater diameter for the oscillating film for H = 2.0 (Fig. 4 (b)) lies close to the maximum values for the steady film, which is also the case for isopropanol (H = 1.0 and H = 2.0 in Fig. 5). Furthermore, in Fig. 4 (b) it can be seen that until the maximum crater diameter is reached, the crater diameter increases symmetrically with respect to the vertical middle line, implying the crater grows symmetrically in radial direction in agreement with drop impact onto a steady film. Only for H = 0.5 for isopropanol a large difference of about one drop diameter can be seen between the two crater maxima, as for the impact onto the oscillating film the crater grows a lot slower and reaches therefore also a lower maximum.

After reaching the maximum crater diameter, the crater begins a receding motion driven by capillary forces. It can be seen in Fig. 2 and 3 that the crater shape changes from hemispherical in the advancing motion to conical during the receding motion. In the case of drop impact onto a steady, non-moving film, the crater is symmetric at the time instant it reaches its maximum diameter, which results in a symmetrical receding motion. This means that the dimensionless diameter at the left side and at the right side with respect to the middle point of the crater is the same. For the cases H = 2.0, We = 151 and Re = 309 (Fig. 4 (b)) of glycerine/water and for H = 1.0, We = 539 and Re = 2010 (Fig. 5) of isopropanol the total crater diameter, as well as the left and right side of the crater, during the receding phase follows almost perfectly the ones measured for impact onto the steady film for the same settings, thus being symmetric. This is also to be expected, as the drops in

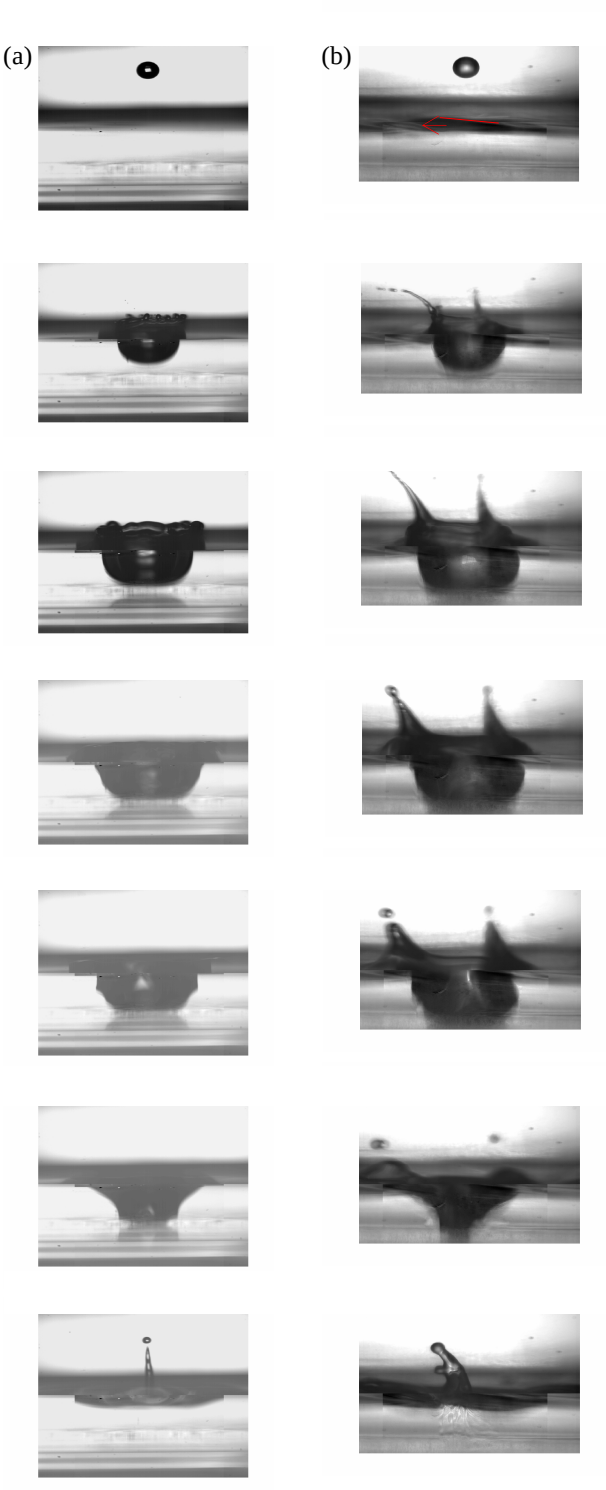

Figure 3. Crater shape for drop impact of isopropanol: (a) steady film ($\overline{H}$ = 2, We = 527, Re = 1,982) and (b) oscillating film ($\overline{H}$ = 2, We = 552, Re = 2,060), T = -2.76, 4.30, 12.98, 23.25, 28.39, 37.71 and 50.88

these two cases impact almost exactly at the bottom of a surface wave.

When the recordings for H = 2.0, We = 291, Re = 419 and H = 2.0, We = 444, Re =524 for glycerine/water just before drop impact are analysed, it is seen that the wave, at which the drops impacts, is for the former a receding surface wave, and for the latter an advancing surface wave, both moving to the left. These inclined, moving waves have a large influence on the crater diameter and its symmetry during the receding motion of the crater. In Fig. 4 (b) it is shown, that the crater diameter for the parameters H = 2.0, We = 291, Re = 419 is symmetric, but that the receding motion of the crater is slower, resulting in a later collapse of the crater, as is the case for impact onto a steady film. For these parameters, three different measurements are analysed, of which the crater diameters are shown in Fig. 6. Although the impact occurs for all three cases onto an inclined and receding surface wave, there are some differences seen for the value of the maximum crater diameter, as well as the crater diameter during its receding phase. For o, for example, there is a small downward step in the crater diameter right after the crater has reached its maximum diameter, resulting from a sharp change of the crater shape as the capillary waves pass the point $y = H/2$. Furthermore, it can be noticed that the spreading of the crater diameter during the receding phase between the different recordings is about half a drop diameter.

For the highest Weber number (H = 2.0, We = 444, Re =524) of glycerine/water, a very asymmetrical receding of the crater is seen, where the right side of the crater recedes much faster than the left side (Fig. 2 and 4 (b)). This can only be explained by the advancing surface wave (red arrow in Fig. 2), due to which the height of the film at the left side of the impacting drop is lower than at the right side. In [12] it was shown, that a larger film height, for the same Weber and Reynolds number, results in a faster and steeper receding and collapse of the crater, as is also seen here. After the collapse of the crater, this asymmetric crater receding motion results in a jet, sharply bent to the left, which slowly erects in time.

For isopropanol (H = 0.5, We = 557, Re = 2108 and H = 2.0, We = 552, Re =2060, Fig. 3 and 5), a large difference between the crater diameter for impact onto a steady and onto an oscillating film is seen. For the lowest film thickness this starts already during the growing period of the crater, resulting in a maximum crater diameter that is one drop diameter smaller for the oscillating film. This difference grows during the crater receding period, as the crater for the oscillating film recedes sooner and faster, resulting in a time difference for the contraction of the crater of about ΔT = 15. The

same differences during the receding period of the crater are seen for the highest film thickness (Fig. 5), although the differences are smaller. For the last case, the drop impacts onto a receding wave (red arrow in Fig. 3), but instead of a larger diameter as is found for H = 2.0, We = 291, Re = 419 (glycerine/water), here a smaller crater diameter is found for the oscillating film.

Conclusions

In this paper the dynamics of the crater formed upon impact of a single drop onto an oscillating, moving film were investigated, using experimental measurements. We focused hereby on the evolution of the crater shape formed beneath the surface upon impact, its depth and crater diameter change with time. These evolutions were compared with drop impacts onto a steady, non-moving film under the same conditions.

It was found, that for all liquids, film heights and Weber numbers, the crater penetrates with constant velocity and reaches the bottom of the film faster when the film is oscillating. When the drop impacts onto the bottom or the top of the surface wave, there is almost no difference between the results for the steady and oscillating film, i.e. the crater evolves in a symmetrical way. In case of an impact onto a receding or advancing inclined wave, the growth and receding phase of the crater in radial direction is either slower or faster, resulting in a lower or higher value for the maximum crater diameter, compared to impact onto a steady film. Furthermore, the crater evolves radially in an asymmetric way, resulting in a sharp inclined jet after collapse.

Nomenclature

D	drop diameter
f	frequency
H	dimensionless film depth
h	film depth
L	amplitude
Oh	Ohnesorge number
Re	Reynolds number
T	dimensionless time
t	time
U	drop velocity
We	Weber number
y	vertical distance from free surface
μ	dynamic viscosity
ρ	density
σ	surface tension

Subscripts

e	exciter

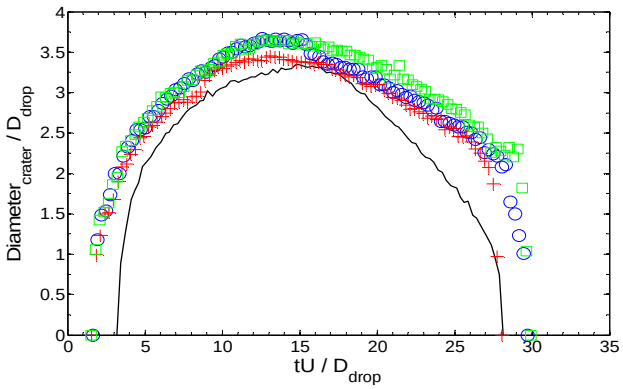

Figure 6. Comparisons of dimensionless crater diameter for three drop impacts of isopropanol under the same impact conditions (steady: - H = 2.0, We = 308, Re = 434; oscillating: o H = 2.0, We = 287, Re = 416; + H = 2.0, We = 293, Re = 423; □ H = 2.0, We = 291, Re = 419)

References

1. Möller, T.J., Chaves, H., and Obermeier, F., *International Spring Fuels & Lubricants Meeting*, Dearborn, Michigan, USA, May 1996, pp. 1-8
2. Stanton, D.W., and Rutland, C.J., *International Congress & Exposition*, Detroit, Michigan, USA, February 1996, pp. 29-45
3. Schünemann, E., Fedrow, S., and Leipertz, A., *SAE Technical Paper Series* 982545:1-9 (1998)
4. Han, Z., Xu, Z., and Trigui, N., *Int. J. Engine Research* 1:127-146 (2000)
5. Levin, Z., *Journal of atmospheric sciences* 28:543-548 (1971)
6. Urban, J., Weigand, B., Roth, N., Eyselein, M., Trackl, K., Tatschl, R., and Raulot, A., Sixth International Conference on Multiphase Flow, Leipzig, Germany, July 2007, pp. 1-9
7. Chigier, N., *Polymeric materials science and engineering* 83:325 (2002)
8. Satas, D., *Web processing and converting technology and equipment*, Van Nostrand Rheinhold, 1984
9. Stanton, D.W., and Rutland, C.J., *Int. J. Heta Mass. Tran.* 41:3037-3054 (1998)
10. Mundo, C., Sommerfeld, M., and Tropea, C., *Atomization and Sprays* 8:625-652 (1998)
11. Bai, C., Rusche, H., and Gosman, A.D., *Atomization and Sprays* 12:1-27 (2002)
12. Berberović, E., Van Hinsberg, N.P., Jakirlić, S., Roisman, I.V. and Tropea, C., *Phys. Rev. E.* 79: 036306 (2009)